



**HAL**  
open science

# Current progress in positive and negative ion modes of a laser ionization mass spectrometer equipped with CosmOrbitrap development - Applicability to in situ analysis of ocean worlds

B. Cherville, L. Thirkell, B. Gaubicher, F. Colin, Christelle Briois

## ► To cite this version:

B. Cherville, L. Thirkell, B. Gaubicher, F. Colin, Christelle Briois. Current progress in positive and negative ion modes of a laser ionization mass spectrometer equipped with CosmOrbitrap development - Applicability to in situ analysis of ocean worlds. *Planetary and Space Science*, 2023, pp.105675. 10.1016/j.pss.2023.105675 . insu-04057408

**HAL Id: insu-04057408**

**<https://insu.hal.science/insu-04057408>**

Submitted on 4 Apr 2023

**HAL** is a multi-disciplinary open access archive for the deposit and dissemination of scientific research documents, whether they are published or not. The documents may come from teaching and research institutions in France or abroad, or from public or private research centers.

L'archive ouverte pluridisciplinaire **HAL**, est destinée au dépôt et à la diffusion de documents scientifiques de niveau recherche, publiés ou non, émanant des établissements d'enseignement et de recherche français ou étrangers, des laboratoires publics ou privés.

# Journal Pre-proof

Current progress in positive and negative ion modes of a laser ionization mass spectrometer equipped with CosmOrbitrap development - Applicability to *in situ* analysis of ocean worlds

B. Cherville, L. Thirkell, B. Gaubicher, F. Colin, C. Briois

PII: S0032-0633(23)00044-2

DOI: <https://doi.org/10.1016/j.pss.2023.105675>

Reference: PSS 105675

To appear in: *Planetary and Space Science*

Received Date: 12 December 2022

Revised Date: 17 March 2023

Accepted Date: 18 March 2023

Please cite this article as: Cherville, B., Thirkell, L., Gaubicher, B., Colin, F., Briois, C., Current progress in positive and negative ion modes of a laser ionization mass spectrometer equipped with CosmOrbitrap development - Applicability to *in situ* analysis of ocean worlds, *Planetary and Space Science* (2023), doi: <https://doi.org/10.1016/j.pss.2023.105675>.

This is a PDF file of an article that has undergone enhancements after acceptance, such as the addition of a cover page and metadata, and formatting for readability, but it is not yet the definitive version of record. This version will undergo additional copyediting, typesetting and review before it is published in its final form, but we are providing this version to give early visibility of the article. Please note that, during the production process, errors may be discovered which could affect the content, and all legal disclaimers that apply to the journal pertain.

© 2023 Published by Elsevier Ltd.



# Current progress in positive and negative ion modes of a laser ionization mass spectrometer equipped with CosmOrbitrap development - applicability to *in situ* analysis of ocean worlds

Cherville B., Thirkell L., Gaubicher B., Colin F., Briois C.

## Abstract

Since the beginning of the space era, mass spectrometry is a reliable technique for *in situ* characterisation of ions and molecules detected in various planetary environments. It has been crucial for the analysis of compounds found in ocean worlds vicinity, such as Enceladus' plumes. The study of the chemical complexity of the environments of the ocean worlds would benefit from the design of a new generation of instruments to allow an exhaustive characterization of them. Among the many objectives of space missions is the search for potential chemical biosignatures on ocean worlds. The precise and unequivocal identification of these biosignatures would be done by mass spectrometers able to perform analyses with a high mass resolving power and high mass accuracy. Efforts are on-going to develop for future space explorations High Resolution Mass Spectrometer instruments (Arevalo et al., 2020) with a space qualified version of the Orbitrap mass analyser, the CosmOrbitrap. Coupled with a commercial laser ionisation source, it has demonstrated promising performances in positive ion mode in terms of mass resolution, mass accuracy and isotopic ratio measurements. This work focuses on the performance achievements with the negative ion mode recently implemented. A study has been performed with a ruggedized spaceflight CosmOrbitrap mass analyser at technical readiness level of 5 at the dual ion polarity to determine the efficiency of the instrument to detect and identify organic molecules of prebiotic interest when embedded in magnesium and sodium salts matrix. These results illustrate the potential of the CosmOrbitrap mass analyser for future *in situ* analysis of ocean worlds as Europa and Enceladus.

## • Introduction

The exploration of the Solar System by robotic spacecraft has revealed the presence of numerous ocean worlds notably that are under the surface ice crust of many moons and dwarf planets (*e.g.* Hussmann *et al.*, 2006; Khurana *et al.*, 1998; Nimmo *et al.*, 2016; Waite Jr *et al.*, 2009). These subsurface oceans provide local conditions suitable for the sustenance of Life as we know it, and that may be close to the conditions of appearance of Life on the early Earth (Camprubí *et al.*, 2019; Johnson and Wing, 2020). To this end, they are among the potentially habitable worlds, which makes them prime targets for astrobiological missions (Hand *et al.*, 2020). In the forthcoming years, both ESA and NASA agencies will launch mission that will explore Europa, a confirmed ocean world with a 100 km thick global liquid ocean at the interface between a surface ice layer and a silicate mantle (Kivelson *et al.*, 2000; Pappalardo *et al.*, 1999). JUICE (Jupiter Icy Moons Explorer), the first ESA's L1 mission, aims, among other objectives, to assess the habitability of Jovian icy moons through multiple flybys of Europa, Callisto and Ganymede and Jupiter system formation mechanisms (Grasset *et al.*, 2013). The JUICE probe will be orbiting Ganymede during the second phase of the mission to deeply characterize this ocean world, which shows strong insights for an internal ocean (Saur *et al.*, 2015). NASA's Europa Clipper Flagship mission which is dedicated to explore Europa has three objectives: the characterization of the ice sheet and of the composition of the subsurface water reservoir, their heterogeneity, the properties of the ocean and the nature of surface-ice-liquid water exchanges; the characterization of the ocean composition and chemistry; the investigation of the processes of surface figure formation, including sites of recent activity (Howell and Pappalardo, 2020). An exhaustive exploration program of ocean worlds of the Solar System has been identified in 2019 by the NASA Outer Planets Assessment Group (OPAG) Roadmaps to Ocean Worlds (ROW) group the priorities for (Hendrix *et al.*, 2019). The goals for the future exploration of known ocean worlds are to characterize the ocean and the habitability of each of them, as well as the potential biosignatures. The NASA/Dragonfly mission, whose objective is the comprehensive exploration of

the surface and lower atmosphere of Titan, has been selected in 2019 as the 4<sup>th</sup> mission of the New Frontiers program. The exploration of Enceladus is also studied, a large number of publications discussed about the future exploration of this moon, such as white papers for the Voyage 2050 long-term plan in the ESA Science Program (Choblet *et al.*, 2021; Mitri *et al.*, 2021; Sulaiman *et al.*, 2021), and mission concepts proposed to NASA in the New Frontiers program (MacKenzie *et al.*, 2021), in the Discovery program (Reh *et al.*, 2016; Tsou *et al.*, 2012), and in response to calls for ESA L-class AO (Coustenis *et al.*, 2009; Tobie *et al.*, 2014).

Among methods that could be used to detect molecular biosignatures and indicators of habitability of ocean worlds, *in situ* mass spectrometers are key instruments (*e.g.* Postberg *et al.*, 2018; Waite *et al.*, 2017 for Enceladus). Moreover, to determine unambiguously the nature of the molecules detected, high mass resolution is certainly great enhancement, even if isotopic pattern can also be a useful tool to discriminate possible molecular candidates within a mass spectrum. Space high resolution mass spectrometry, capable of deciphering isobaric interferences, could be crucial in the identification of molecular biosignatures. Among the technologies used by high mass resolution laboratory mass spectrometer is the Orbitrap<sup>TM</sup> technology. The adaptation of the Orbitrap technology for *in situ* space applications is led by a consortium of 6 laboratories (Laboratoire de Physique et de Chimie de l'Environnement et de l'Espace (Orléans, France), Laboratoire Atmosphères, Milieux, Observations Spatiales (Guyancourt, France), Laboratoire inter-universitaire des systèmes atmosphériques (Créteil, France), Institut de Planétologie et d'Astrophysique de Grenoble (Grenoble, France), Centre de Sciences Nucléaires et de Sciences de la Matière (Orsay, France), J. Heyrovsky Institute of Physical Chemistry (Prague, Czech Republic)), in partnership with the French space agency (Centre National d'Études Spatiales, CNES) and ThermoFisher Scientific (Briois *et al.*, 2016). This development aims to create a space mass analyzer called CosmOrbitrap, including a D30 Orbitrap cell; the standard Orbitrap cell in (Makarov *et al.*, 2009). Therefore, bringing the Orbitrap technology into space is not only to develop a space-ruggedized cell, but also an R&T development effort dedicated to its electronics: a low noise pre-amplifier (PA), an ultra-stable High-

Voltage (HV) power supply and data processing Fourier Transform system as illustrated in Figure 1. To be highly performing and considered to be integrated in any future space mission, a bottleneck of level 5-6 high standard of Technological Readiness Level (TRL) has to be reached. This level corresponds to a model demonstration in relevant environment; lower levels correspond to formulation of principles and proof-of-concepts experiments.

To determine the CosmOrbitrap prototype capabilities, it has been coupled directly to a commercial Nd:YAG laser ionization source using a fourth harmonic generator to produce a 266 nm wavelength laser pulse (Briois *et al.*, 2016 ; Selliez *et al.*, 2019). This CosmOrbitrap-based LIMS (Laser Ionisation Mass spectrometer), hereafter called LAb-CosmOrbitrap, has demonstrated in positive ion mode its ability to characterize a variety of planetary analogs, samples of astrobiological interest as amino acids at low level concentrations ( $\leq 1$  pmol/mm<sup>2</sup>) (Arevalo Jr. *et al.*, 2018), and complex samples as tholins with a single laser shot experiment (Selliez *et al.*, 2020), with performance similar to the one obtained with commercial ThermoFisher instruments using D30 Orbitrap cell. Since then, efforts have been conducted to ruggedize the spaceflight TRL level of the CosmOrbitrap to level 5; this level has been awarded to the CosmOrbitrap development by a committee of experts from CNES in an end-of-R&D review.

CosmOrbitrap R&D development is included in three complete instruments, whose development is led by collaborators from the University of Maryland (US) and the NASA Goddard Space Flight Center. The two first instrument are Characterization of Ocean Realms And Life Signatures (CORALS, PI: R. Arevalo, Univ. of Maryland) and Characterization of Regolith And Trace Economic Resources for lunar surface exploration (CRATER, PI: R. Arevalo, Univ. of Maryland). Both instruments include the CosmOrbitrap analyzer and a direct laser ionization system, and are funded respectively by the NASA-ROSES (Research Opportunities in Space and Earth Sciences)/ICEE-2 (Instruments Concepts for Europa Exploration) and NASA-ROSES/DALI (Development and Advancement of Lunar

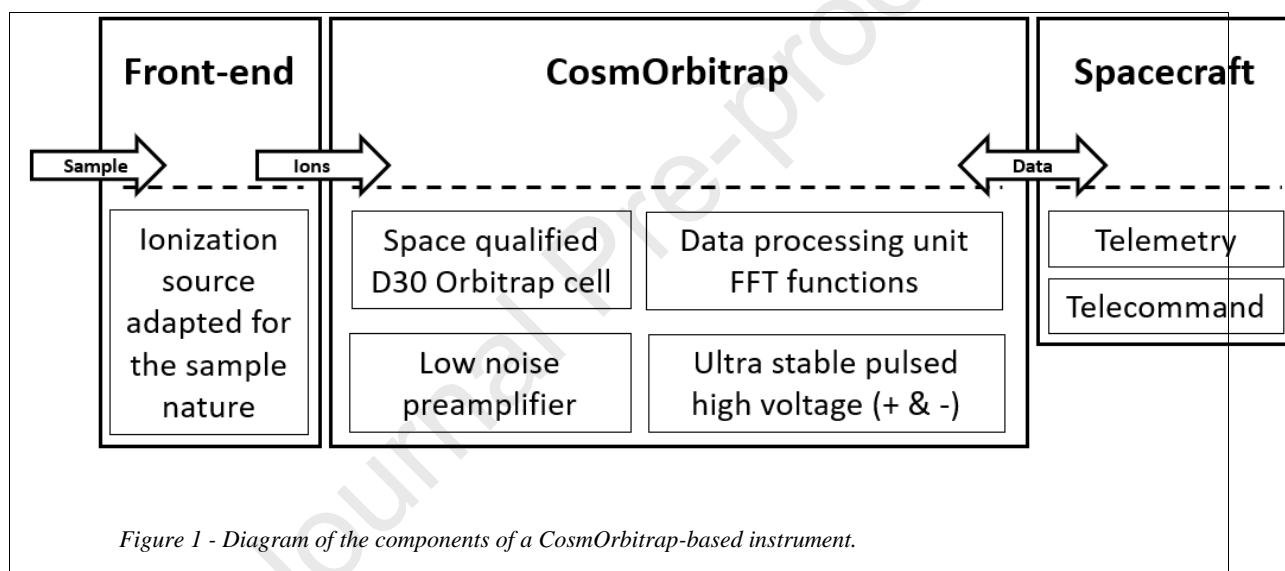
Instrumentation) programmes. The third instrument is Advanced Resolution Organic Molecular Analyzer (AROMA, PI: A. Southard, GFSC), funded by the NASA-ROSES/MatISSE (Maturation of Instruments for Solar System Exploration) programme. This instrument is a more complex one, including an electron impact and a laser ionization system. Those instruments promise innovative results and mark a new step in the field of high-resolution mass spectrometers dedicated to space exploration.

To this end, a SWaP (Size Weight and Power) Orbitrap-based LIMS instrument integrating the CosmOrbitrap has been developed by R. Arevalo team in collaboration with the CosmOrbitrap consortium. This instrument aims to prove relevancy of an Orbitrap-based instrument for life detection objectives and lunar exploration; it is described in Arevalo *et al.*, 2023.

Undeniably, the previous missions to ocean worlds taught us how both negative and positive ion modes would give complementary scientific information when analyzing a complex sample such as minerals or organic molecules mixture (e.g. Waite *et al.*, 2007). For example, the detection of high mass negative ions in Titan's upper atmosphere with the Cassini Plasma Spectrometer and the identification of low mass positive ions with the Ion and Neutral Mass Spectrometer have been necessary to model the formation of the aerosols in the atmosphere (Waite *et al.*, 2007). The study of Titan's aerosols analogues also shows that positive and negative ion modes are complementary for the characterization of this kind of complex samples (Somogyi *et al.*, 2012). Some features of the ocean worlds, such as the presence of Na- and Mg-bearing sulfite and chloride material at their surface (Brown and Hand, 2013; Ligier *et al.*, 2016; Trumbo *et al.*, 2019), may require both polarities for a comprehensive characterization.

The availability of both modes with the same capabilities appears therefore to be crucial for space exploration mass spectrometry instrument with astrobiological objectives. In order to offer dual ion polarity capability, negative ion mode has newly been implemented in our LAB-CosmOrbitrap

instrument. Performances in term of mass resolution, mass accuracies and relative isotopic error are presented in the sub-section 3.1 of this paper. The sub-section 3.2 focuses on the effect of a modification of the hardware, from a commercial HV power supply to the TRL5 one, specially developed for this instrument. The sub-section 3.3 intends to demonstrate how the fragmentation pattern obtained during the analysis of a nucleoside with the LAb-CosmOrbitrap instrument in its TRL5 configuration can lead to identification of the molecule. It also intends to show the effect of a salt matrix on this identification process.



- **Experimental setup**

### 2.1. Laser Ablation-CosmOrbitrap mass spectrometer overview

The LIMS set up used in this work is a laser ablation CosmOrbitrap mass spectrometer, hereafter called LAb-CosmOrbitrap developed at Orleans in the Laboratoire de Physique et Chimie de l'Environnement et de l'Espace (LPC2E). LIMS is a destructive method: the laser removes a part of the sample and ionizes it. This destruction process can be modulated by varying the laser output

energy. Extensive review of LIMS technique can be found in Azov *et al.* (2020) and references therein.

As illustrated in Figure 2, LAb-CosmOrbitrap is a compact instrument that used solid state UV (266 nm) laser ionization system directly connected, through an ion optics system, to the Orbitrap cell. Green elements reported in Figure 2 compose the R&T CosmOrbitrap development efforts. Details of the sample holder, pumping, ion optics system, principle of the orbitrap cell, and operation of the data acquisition have been fully described in Briois *et al.* (2016) and Selliez *et al.* (2019).

Since these previous studies, some modifications of the set-up have been performed:

i) in the present work, the laser is a pulsed UV Nd-YAG laser (Q-smart 450, Quantel) operating at the fourth harmonic (266 nm wavelength, 4 ns pulse width, 10 Hz). The laser beam is sampled thanks to a beam splitter (BSF10-UV, Thorlabs) and its energy is controlled by a rotating polarizer (can vary from 1 to 400  $\mu\text{J}$  per pulse). An Ophir PE9-SH power meter measures the laser beam energy. As in previous works (Briois *et al.*, 2016), (Arevalo Jr. *et al.*, 2018; Selliez *et al.*, 2020, 2019), the laser beam reaches the sample with an incident angle of  $50^\circ$ , resulting in an elliptical footprint of around  $30\ \mu\text{m}$  over  $40\ \mu\text{m}$  (measured on silicon wafer) and energy density of from  $0.27\ \text{J}\cdot\text{cm}^{-2}$  to  $10.61\ \text{J}\cdot\text{cm}^{-2}$ .

ii) negative ionization mode has been implemented. A pulsed high voltage power supply that delivers the initial voltage ramp followed by a stable HV plateau during the acquisition time (typically 1 s), polarizes the Orbitrap mass analyzer central electrode. Switching from positive ion mode to negative ion mode is done by inverting the polarity of the high voltage power supplies.

iii) and finally, experiments have been performed with a leverage version of technical readiness level of the CosmOrbitrap development (all the green elements reported in Figure 2: ruggedized orbitrap cell, low noise pre-amplifier and dual ion mode ultra-stable pulsed high voltage).

The pre-amplifier used for experiments presented in sub-section 3.1 is an under-development in-house device that is a preliminary version of the space-qualified pre-amplifier used for experiments presented in sub-sections 3.2 and 3.3.

Fast Fourier Transform (FFT) had been applied on a portion of the signal measured by the pre-amplifier, after an optional zero-padding step and application of an apodisation function (*e.g.* Brenna and Creasy, 1989). The resulting frequency spectrum is calibrated and converted to a mass spectrum (Perry *et al.*, 2008).

In these studies, mass calibration was made on the most intense peak of the 10-500  $m/z$  range (usually  $m/z = 114.9033$  ( $\text{In}^+$ ) in positive ion mode and  $m/z = 26.0036$  ( $\text{CN}^-$ ) in negative ion mode). But, when a deviation in the mass accuracy is visible on a single spectrum, a two-points calibration is applied. In that case, calibrants are two intense peaks of the frequency spectrum, separated by a minimum of 100 kHz. The range [0.4 ; 1.7] MHz roughly corresponds to the [12 ; 300]  $m/z$  range. A calibration factor is calculated for both peaks, and a linear regression is applied, resulting in a calibration factor varying linearly in function of the frequency. Using this calibration factor gave us a better mass accuracy for a single laser shot experiment. All the spectra shown in this article were issued from Matlab™ scripts developed in-house, allowing optional zero-filling and apodization, as well as further data treatments. The data acquisition system has been supplied by the Alyxan company (Orsay, France). It consists of a data acquisition board (Acquitek CH-3160, 40 MS/s, 12 bits), sampling the signal at 5 MHz and recording  $2^{22}$  points, allowing recording of transients of maximum length of 838 ms in this configuration. A National Instrument CompactRIO coupled with a custom LabView software delivers the trigger signals that allow the synchronization of the laser pulse, the Orbitrap central electrode high voltage switch and the acquisition system.

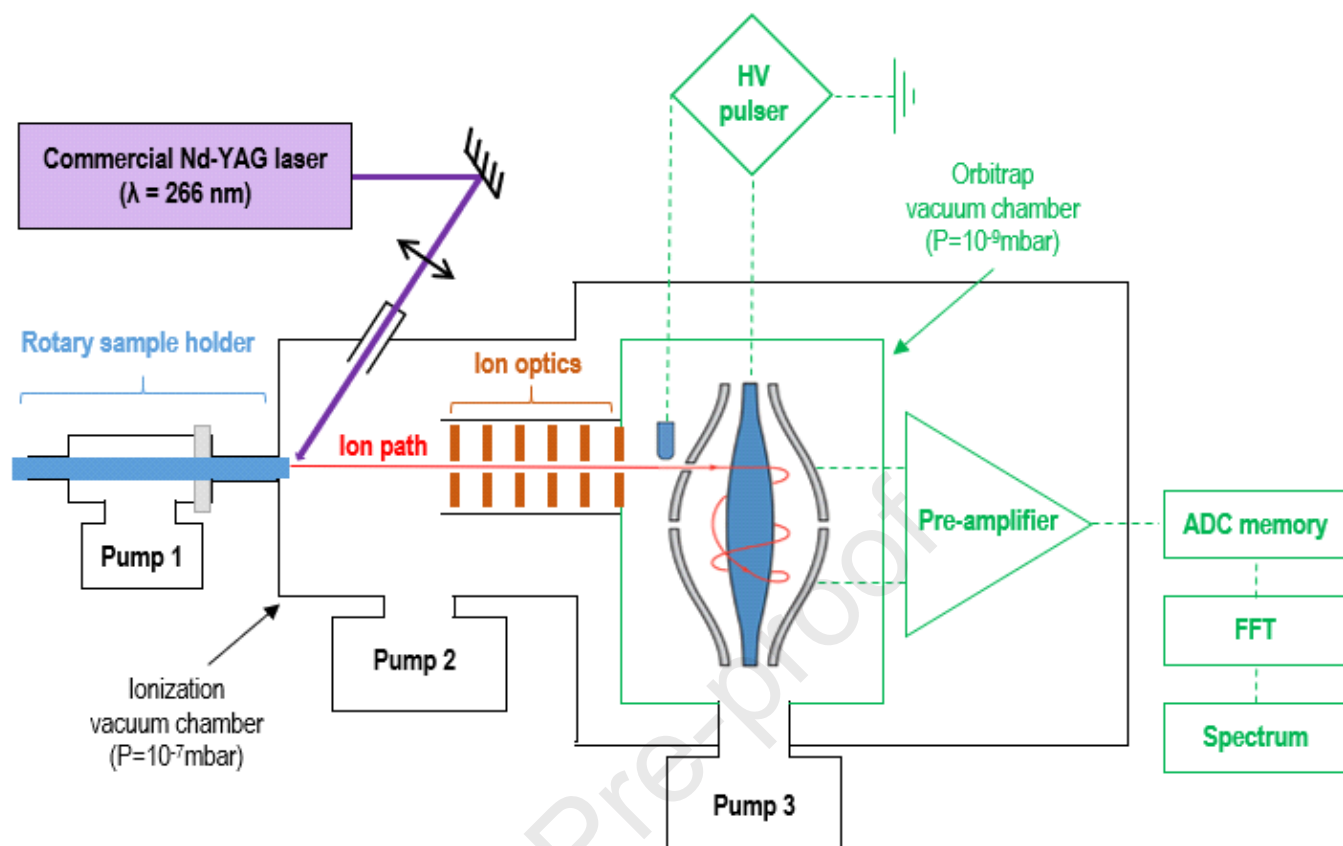


Figure 2 - Scheme of the LAB-CosmOrbitrap instrument. Green parts are CosmOrbitrap elements under development, other parts are commercial elements.

### • Sample Materials and Preparation

To validate the analytical performances of the instrument in negative ion mode, experiments were performed on a set of four high electron affinity metallic samples, one halide salt and two small organic compounds.

Detection of negative ions in mass spectrometry, is more challenging than detection of positive ions. In negative ion mode, signal amplitude is severely reduced compared to that observed in the positive ion mode. To have a chance to detect metallic anions, high electron affinity (EA) elements have been chosen (Myers, 1990).

Pure gold (Au, EA(Au) = 2.309 eV), pure platinum (Pt, EA(Pt) = 2.128 eV), and a silver/copper alloy ( $\text{Ag}_{0.72}\text{Cu}_{0.28}$ , EA(Ag) = 1.302 eV, EA(Cu) = 1.128 eV) were selected for this study. Due to the fact that laser ionization is destructive method, plain metallic samples have been privileged; they are therefore more resilient under the laser shot than could be any powdered compounds.

The halide salt sample, caesium triiodide ( $\text{CsI}_3$ ) was chosen due to high electron affinity of iodide ion I<sup>-</sup>.

The two organic compounds investigated in these studies are i) a purine base (Adenine,  $\text{C}_5\text{N}_5\text{H}_5$  (Sigma Aldrich; )), and ii) a model of small peptide (TriGlycine,  $\text{C}_6\text{H}_{11}\text{N}_3\text{O}_4$  (Sigma Aldrich; )). Glycine and Adenine are moreover easily detectable in negative ion mode. Metallic sample were delivered in thin foil of high purity (Goodfellow; ). Small pieces of each metallic foil samples were cut, then cleaned with HPLC-grade acetone and n-hexane to avoid traces of residual oils from manufacturing process, and then pressed onto a circularly shaped Indium plate (Goodfellow ). Halide salt and organic compounds were delivered in powders form and have been homogenized using an agate mortar and pestle. No chemical preparation was done prior to the analysis. For each, few mg of sample has been deposited onto the surface of a Indium plate, then pressed using an agate pestle. Thickness is estimated to be less than 100  $\mu\text{m}$ . For each experiment, prior cleaning of agate mortar, pestle and sample plate have been performed using HPLC-grade acetone and n-hexane.

To prospect the effect of salts on the detection of biogenic samples, a set of two samples were investigated, including pure Adenosine ( $\text{C}_{10}\text{H}_{13}\text{N}_5\text{O}_4$ ; Sigma Aldrich; ), and Adenosine mixed with two inorganic salts, magnesium sulfate ( $\text{MgSO}_4$ ; Sigma Aldrich; ) and halite ( $\text{NaCl}$ ; Sigma Aldrich; ) in the following proportion : 10 wt% of pure organic (molar fraction: 6.25%), 45 wt% of  $\text{MgSO}_4$  (molar fraction: 31.25%) and 45 wt% of  $\text{NaCl}$  (molar fraction: 62.5%). All these samples were delivered in powder form and have been prepared following the same procedure as the halide salt. Same cleaning procedure of the agate mortar, pestle and sample plate prior the deposit has been performed as described above.

- **Results**

### **3.1 Validation of the performance in negative ion mode of the LAb-CosmOrbitrap**

To determinate the capabilities of our LAb-CosmOrbitrap set-up in both ion polarities, a series of experiments have been performed with the newly implemented negative mode. All these tests were performed using commercial HV power supply to serve as reference.

During the ionization process, in additions of ions, many electrons are generated. In negative ion mode, these electrons are repelled from the sample holder due to the negative bias applied to it. When the density of electrons is too high, an electrical discharge between the first lens and the sample holder takes place, which prevents the correct extraction of ions. Therefore, when analyzing negative ions, to avoid electric discharges between the ion optics and the sample holder, we found experimentally that the laser beam energy has to be reduced to  $<100 \mu\text{J}/\text{pulse}$ . As a consequence, in negative ion mode, the signal amplitude is reduced compared to the amplitude observed in the positive ion mode. The data presented in this sub-section have been obtained from on a reduced portion of the acquired signal (300 ms) to select the part containing relevant data to maximize the signal-to-noise ratio (SNR) of the peaks.

#### ***Mass resolution***

Figure 3 shows the mass resolving power as a function of mass to charge ratio obtained with the LAb-CosmOrbitrap in negative ion mode for the metallic samples, the halide salt and the tripeptide studied. Data have been recorded with a 300 ms-long transient and a sampling rate of 5 MHz at a total pressure lower than  $10^{-8}$  mbar, measured with Pfeiffer cold cathode gauge (Pfeiffer IKR 270). The gauge is pumped through a device designed to have a conductance similar to the one associated

to the D30 Orbitrap cell. A model calculated with Comsol MultyPhysics software confirmed that at equilibrium, pressure measured by the gauge is close to the pressure inside the Orbitrap Cell to a factor of 2 or 3. The data presented come from a single spectrum for TriGlycine fragments, and for most of the metal samples. For each analysis, a zero padding of 4 was applied.

The mass spectra of the analysis of Platinum in negative ion mode show the 4 more abundant stable isotopes. Due to the low intensity of the signal, the theoretical amplitude of the peaks of  $^{190}\text{Pt}^-$  and  $^{192}\text{Pt}^-$  is lower than the mean noise level.

Concerning the TriGlycine sample, the points on the Figure 3 correspond to pseudo-molecular peak  $[\text{C}_6\text{H}_{11}\text{O}_4\text{N}_3 - \text{H}]^-$  and its fragments to which a relevant chemical formula had been successfully attributed ( $\text{C}_\alpha\text{H}_\beta\text{N}_\gamma\text{O}_\delta$ , with  $\alpha \leq 6$ ,  $\beta \leq 12$ ,  $\gamma \leq 3$  and  $\delta \leq 4$ , and a resulting mass measurement error less than 10 ppm. For more details about the chemical attribution method, see section about Mass accuracy).

On the mass range considered, with the short length signal analysis of 300 ms, the mass resolving power varies from 94,000 at nominal  $m/z$  26 ( $\text{CN}^-$  ion, TriGlycine fragment) to 46,000 at  $m/z$  198 ( $^{198}\text{Pt}^-$  ion). The lowest value of the mass resolving power is 35,000 at  $m/z$  144. Evolution of the mass resolving power as a function of  $m/z$  can be fitted by a power law ( $m/\Delta m$  (FWHM) =  $k \cdot (m/z)^{-1/2}$ ), in agreement with the Orbitrap cell resolving power law (Makarov, 2000; Perry *et al.*, 2008). The high variability in mass resolving power values is interpreted as a consequence of the high variability of the SNR of the peaks considered. The data corresponding to high SNR peaks are above the fitted curve, lower SNR peaks are below it; these peaks tend to reduce the mass resolution. We can conclude that an optimization of the ionization enhancing the SNR of the peaks in negative ion mode would increase the mean mass resolution at a given  $m/z$ .

We demonstrate that for the analysis of negative ions in non-optimal conditions, our LAB-CosmOrbitrap instrument mass resolving power fits is close to half of the maximum reachable with

this Orbitrap cell with for the same transient time, despite the fact that our instrumental set-up is much more simplified.

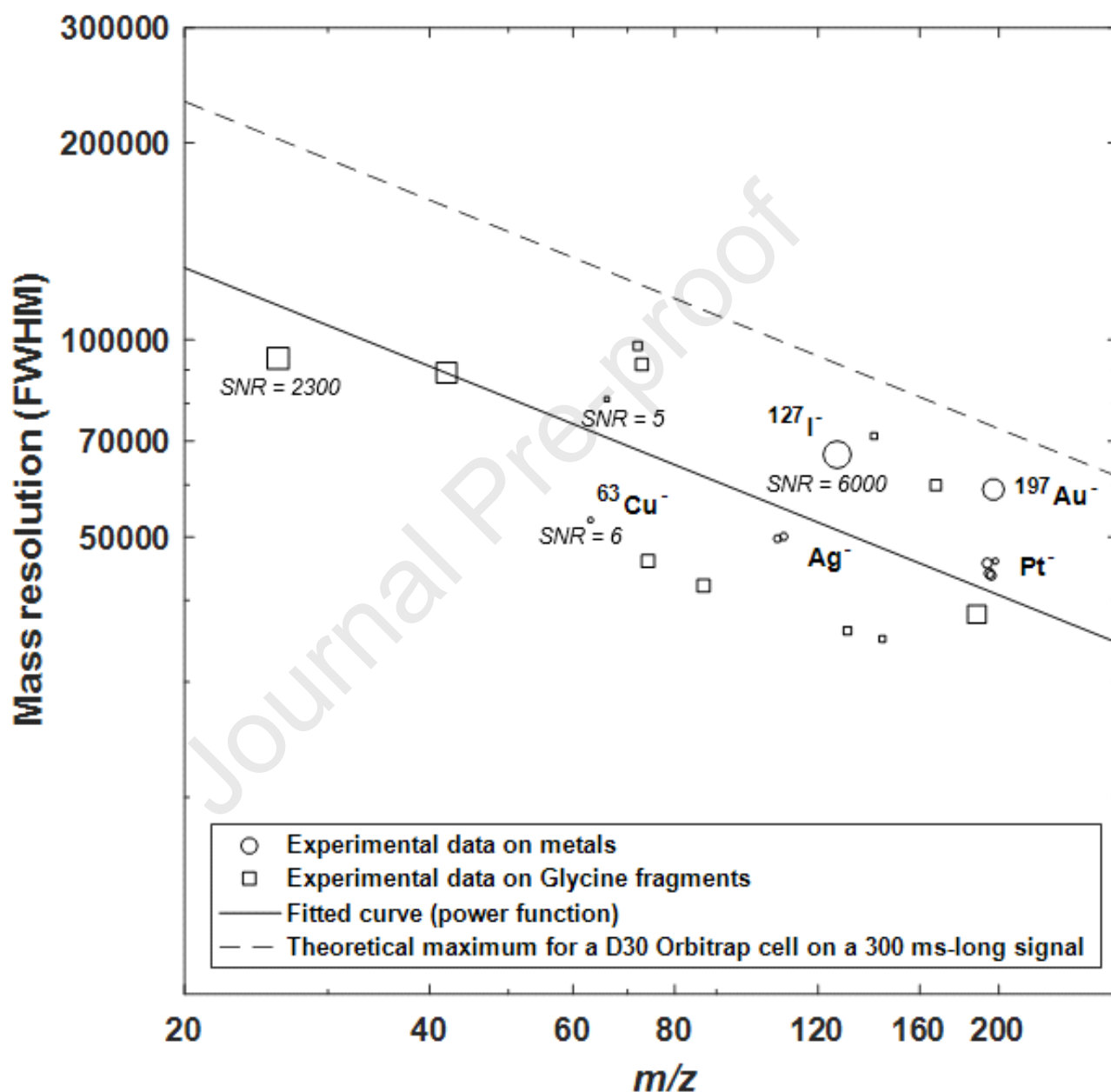


Figure 3 - Mass resolving powers of the LAb-CosmOrbitrap as a function of  $m/z$  on logarithmic scale. The data from single laser shots have been generated by a FT of the transient recorded for 300 ms and a sampling rate of 5 MHz. The circles represent metallic samples. The squares represent TriGlycine sample pseudo-molecular peak ( $m/z = 188.0747$ ) and its detected fragments. The size of the two types of points is proportional to the signal-to-noise ratio of the corresponding

peaks, extreme SNR values for each data set are written. Solid black curve is a fit taken from the data presented here, according to the power function  $y = a * x^m$ . Black dash curve shows the maximum resolution for an emitted spectrum of a 300ms-long signal sampled at 5 MHz.

### **Relative isotopic error**

To determinate the capabilities of our LAB-CosmOrbitrap test bench, we investigate the isotopic pattern of the platinum sample. Top panel of Figure 4 shows a zoom of the  $m/z$  193 to 199 range of a single laser shot mass spectrum. Peaks of the  $^{194}\text{Pt}^-$ ,  $^{195}\text{Pt}^-$ ,  $^{196}\text{Pt}^-$  and  $^{198}\text{Pt}^-$  ions are easily identified, corresponding to the four more abundant stable isotopes of platinum element. The relative isotopic abundancies (RIA) of these 4 isotopes are respectively  $\text{RIA}(^{194}\text{Pt}) = 0.3286$ ,  $\text{RIA}(^{195}\text{Pt}) = 0.3378$ ,  $\text{RIA}(^{196}\text{Pt}) = 0.2521$ ,  $\text{RIA}(^{198}\text{Pt}) = 0.07356$ .  $^{190}\text{Pt}^-$  and  $^{192}\text{Pt}^-$  ions are too low to be detectable on a single laser shot experiment ( $\text{RIA}(^{190}\text{Pt}) = 0.00012$ ,  $\text{RIA}(^{192}\text{Pt}) = 0.00782$ ). The measured RIA of the four isotopes detected is close to the literature standard relative abundance (standard values from the NIST database).

The RIA error (%) had been calculated as shown in Eq. (1) (Knolhoff *et al.*, 2014) from the mean  $\text{RIA}_{\text{exp}}$  of 3 platinum mass spectra for the 4 detected stable isotopes.

(1)

Resulting RIA error values in Figure 4 are less than 5% for the 3 major isotopes, which lies within the threshold stated by Kind and Fiehn (2006) for a reliable chemical identification of organic compounds. However, these results have to be confirmed by the analysis of organic compounds and the quantification of the  $^{13}\text{C}/^{12}\text{C}$  ratio. Such analyses will confirm that the instrument is capable to fulfill the Kind and Fiehn threshold. The standard deviation error bars show a variation of the measurement over 3 independent mass spectra, especially for the  $^{198}\text{Pt}^-$  isotope, due to a low SNR value, increasing uncertainty of the amplitude.

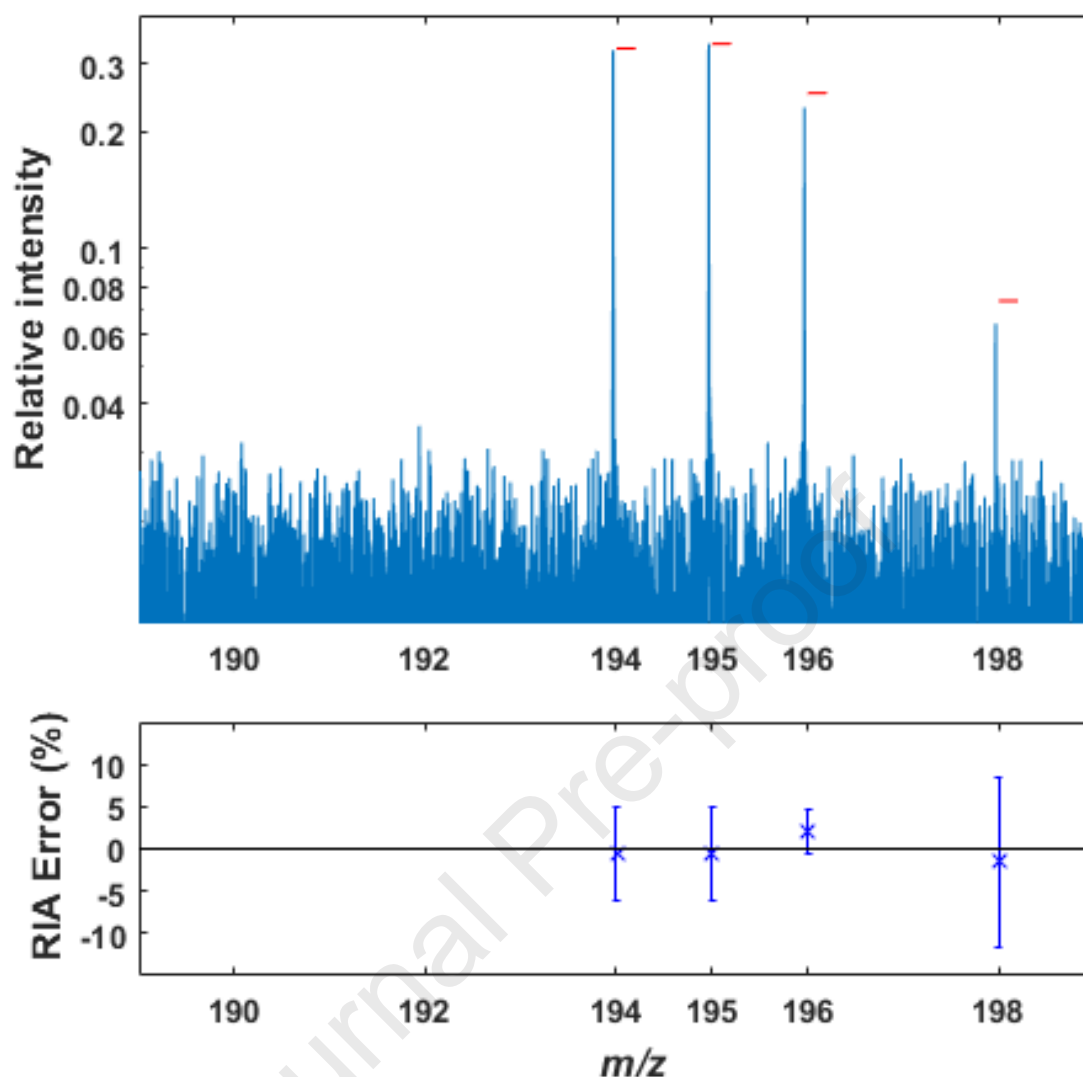


Figure 4 - Platinum sample data recorded for a single laser shot with the LAb-CosmOrbitrap, from a 300 ms-long signal. Top panel: single laser shot negative mass spectrum of platinum. The amplitude has been normalized so that the sum of the amplitudes of the 4 Pt isotopes is equal to 1. Intensity of the x-axis corresponds to the noise level of the spectrum. The red horizontal bars correspond to the literature relative abundance of these 4 isotopes. Bottom panel: deviation on relative abundances of the mean of 3 spectra has been indicated as a function of mass. The error bar is the standard deviation of relative abundances.

### **Mass accuracy and attribution of organic fragments**

An important criterion to verify whether the resulting mass spectra of the instrument allow us to assign consistent chemical formulas to the detected peaks is to evaluate the mass accuracy. This has

been studied in negative ion mode with a pure Adenine sample deposited onto the surface of a Indium plate.

The calibration has been made on the peaks corresponding to  $\text{CN}^-$  and  $\text{C}_5\text{H}_4\text{N}_5^-$  ions. The applied chemical assignment method consists of a peak selection step according to their signal-to-noise ratio (SNR). In the following example, the selected peaks have an  $\text{SNR} > 5$ . The peaks corresponding to the 2nd and 3rd order harmonics of the most intense peaks are removed from the list of considered peaks. Then, the mass corresponding to the peak is compared to a table of possible theoretical masses of molecules. Here, the theoretical masses correspond to molecules of the type  $[\text{C}_\alpha\text{H}_\beta\text{N}_\gamma\text{O}_\delta + \text{In}_\epsilon]^-$ , with  $\alpha, \beta, \gamma \text{ \& } \delta \leq 6$  and  $\epsilon \leq 3$ . The formula  $[\text{C}_\alpha\text{H}_\beta\text{N}_\gamma\text{O}_\delta + \text{In}_\epsilon]^-$  corresponding to the mass closest to the maximum of the selected peak is assigned to the peak, and the resulting mass precision is calculated as shown in equation (2).

(2)

The formula is considered as incorrect if the mass accuracy exceeds a threshold. This criterion is fixed to 20 ppm for the following studies.

In the case where a mass peak  $M$  has been assigned a formula including a carbon atom, if the intensity of the mass peak  $M + 1$  is consistent with the presence of a carbon 13 atom, the formula proposed as assignment can therefore be of the form  $[\text{}^{12}\text{C}_{\alpha-1}\text{}^{13}\text{C}_1\text{H}_\beta\text{N}_\gamma\text{O}_\delta + \text{In}_\epsilon]^+$ .

The capability of the LAb-CosmOrbitrap to give a chemical formula to each peak detected on a positive ions mass spectrum of Adenine ( $\text{C}_5\text{H}_5\text{N}_5$ ) has been evaluated. A spectrum derived from a signal without any apodization window, and a zero padding of 3 is presented in Figure 5. The Fourier transform has been calculated over 25 to 325 ms time range of the acquired signal; the 25 first milliseconds of the signal correspond to acquisition board saturation. In the Figure 5 upper part, 24 among the most intense peaks detected were selected and a chemical formula were assigned according to the method described before. The formula assigned to all these peaks is of the type  $[\text{C}_\alpha\text{H}_\beta\text{N}_\gamma]$ , with  $\beta \leq 4$  and  $\alpha \text{ \& } \gamma \leq 5$ . These formulas are consistent with organic Adenine fragments,

detected in negative ion mode. As seen in the Figure 5 lower part the largest deviations from the exact mass of the assigned compounds are about 3 ppm, while the majority of the points are in the -2 to 2 ppm range. These results are comparable than those obtained by Xu *et al.* (2010) with a commercial Orbitrap LTQ instrument for the mass range 75 to 810 u and without external calibrant. Thanks to this excellent mass accuracy, these data demonstrates the reliability of chemical formulas attribution of a CosmOrbitrap-based instrument.

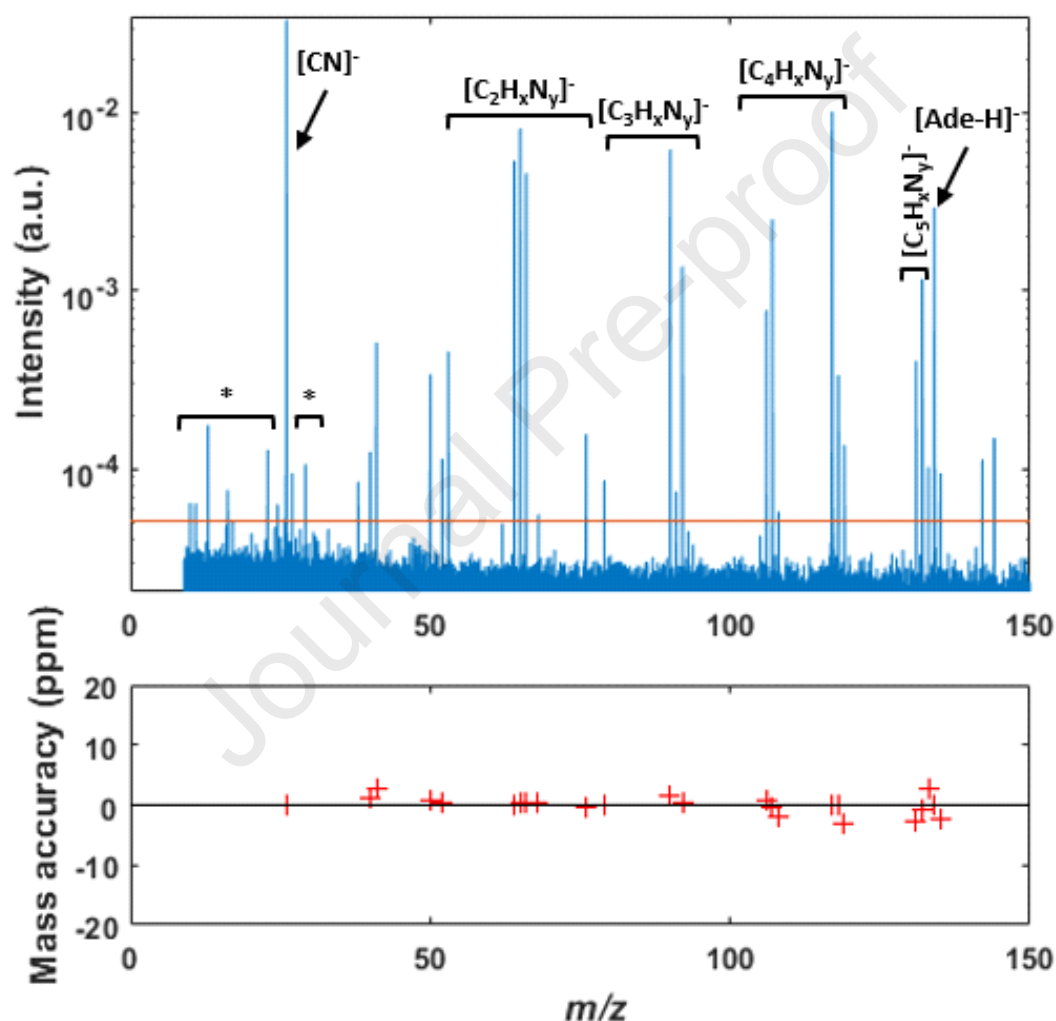


Figure 5 - Lab-CosmOrbitrap Adenine spectrum from a 300 ms-long signal. Top panel: single laser shot negative mass spectrum of Adenine calibrated on  $\text{CN}^-$  and  $[\text{Ade-H}]^-$  peaks. The orange line corresponds to the SNR threshold of 5. // symbol indicates that the peak is not fully showed, the value corresponds to its maximum amplitude. The symbol \* indicates the peaks are attributed to harmonics. Bottom panel: mass accuracy of the identified  $(\text{C}_\alpha\text{H}_\beta\text{N}_\gamma\text{O}_\delta + \text{In}_\epsilon)^-$  molecules corresponding to peaks from the spectrum. Boundaries of the y-axis correspond to the exclusion threshold from the data treatment method.

### 3.2. Verification of the capabilities of TRL5 ruggedized spaceflight CosmOrbitrap development

In light of the good dual polarity performances obtained, a checking of the ruggedized spaceflight CosmOrbitrap efficiency has been then investigated, and particularly on the HV power supply. Therefore, the commercial ThermoFisher HV power supply has been replaced by the TRL5 ruggedized spaceflight HV power supply, and the pre-amplifier has been upgraded to a new version. Identical experiments with Adenine sample deposited onto the surface of an Indium plate have been conducted. For both sets of analysis, the Fourier transform has been calculated over 100 to 838 ms time range of the acquired signal.

A zoom of the peak attributed to respectively  $^{115}\text{In}^+$  and  $[\text{C}_5\text{N}_5\text{H}_5 + \text{H}]^+$  using both HV power supplies are presented in Figures 6-A and -B. Both peaks show a similar width measured at half maximum between measurements with the commercial HV power supply and the TRL5 one, and similar mass accuracy. These data confirm that the integration of the TRL5 HV power supply has not affected the mass resolving power and mass accuracy performances of the LAB-CosmOrbitrap instrument.

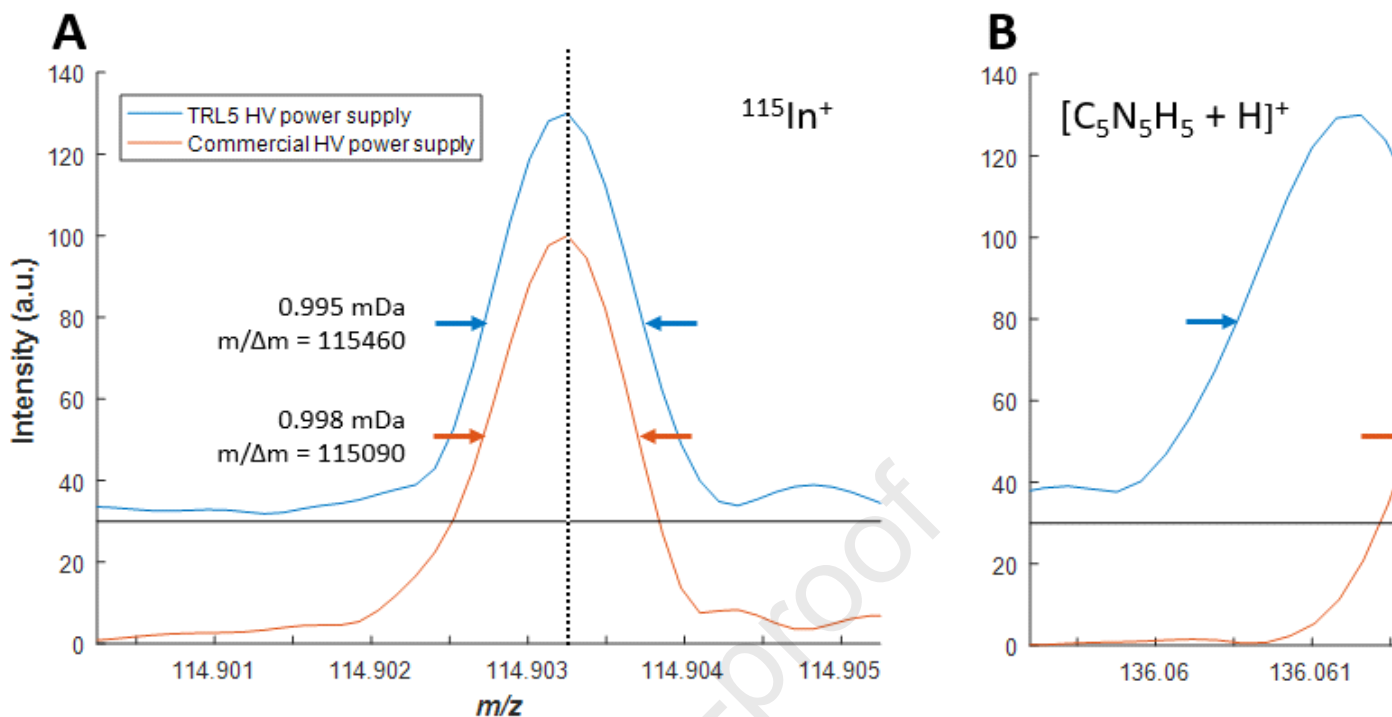


Figure 6 – Mass spectra of Adenine powder calibrated on the peak attributed to  $^{115}\text{In}^+$  obtained with the two HV power supplies. The same experimental setup has been used for each HV power supply. The width of the peaks is measured at 50% of the maximum amplitude; the intensity of the TRL5 HV power supply data has been shifted by 30 for sake of clarity. FFT has been applied on a 738 ms-long signal. Dotted vertical lines correspond to the exact mass of the considered ion. A - detail of the peak attributed to  $^{115}\text{In}^+$  with measured width and mass resolution. B – detail of the peak attributed to  $[\text{C}_5\text{N}_5\text{H}_5 + \text{H}]^+$  molecule with measured width, mass resolution and mass accuracy.

### 3.3. Applicability of a laser-CosmOrbitrap instrument to *in situ* analysis of ocean worlds

Given these high performances obtained with the TRL5 version of the CosmOrbitrap development, and the newly implemented ion mode capability, a study has been performed on both ion polarity with Adenosine sample to determine the efficiency on the detection/identification of simple organic molecules of prebiotic interest when embedded in magnesium and sodium salts matrix.

A Hann apodization function has been applied to the measured signals, as well as a zero-padding of 3. The Fourier transform has been applied over the 100 to 838 ms time range. The chemical formula assignment method described in “*Mass accuracy and attribution of organic fragments*” sub-section has been used, the detected masses were compared to those corresponding to molecules of type  $[C_{\alpha}H_{\beta}N_{\gamma}O_{\delta} + In_{\epsilon}]^{+}$ , with  $\alpha \leq 16$ ,  $\beta \leq 30$ ,  $\gamma$  &  $\delta \leq 6$  and  $\epsilon \leq 3$ .

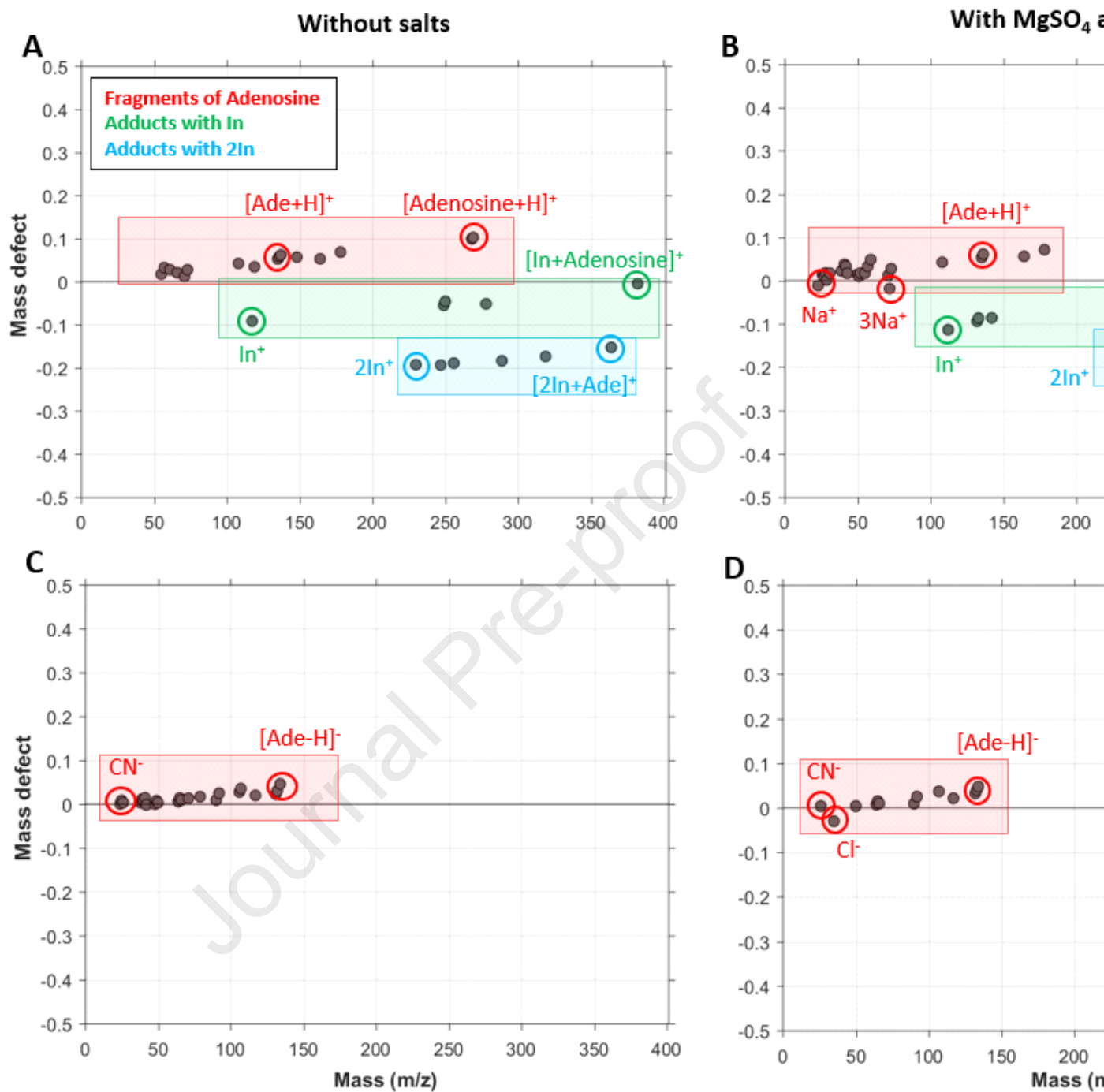
Figure 7 presents as mass defect versus exact mass the results of the 4 set of experiments in different panels. Panels on the right (A and C) are experiments performed without any salts, and those on the left (B and D) are the ones with salts. Top panels (A and B) are experiments performed in positive ion with the LAb-CosmOrbitrap prototype, as bottom panels (C and D) the experiments in negative ion mode.

The mass spectra of experiments performed in positive ion mode (top panels of Figure 7) exhibits three families of peaks according to their mass defect that are outlined with rectangular-shaped areas : i) reddish area corresponding to Adenosine pseudomolecular peak  $[Adenosine + H]^{+}$  and its fragment peaks, ii) greenish area corresponding to adducts between Adenosine molecule or some of its fragments and one In ion, which is the metallic target holder, and iii) blueish area corresponding to adducts with two In of the Adenosine molecule or some of its fragments. Adenosine ( $C_{10}H_{13}N_5O_4$ ) is a ribonucleoside which is composed of Adenine ( $C_5H_5N_5$ , hereafter called Ade in the Figure 7) linked to a Ribofuranose ( $C_5H_{10}O_5$ ) molecule after the loss of  $H_2O$ . In experiments performed without any salt matrix (Figure 7-A), peaks corresponding to characteristic fragments such as  $[Ade + H]^{+}$  are detected, as well as adducts of Ade and In and 2In. When embedded in the salty matrix used for this work (Figure 7-B) no detection of the pseudomolecular peak  $[Adenosine + H]^{+}$  or its adduct with In  $[Adenosine + In]^{+}$  ions were found. Despite the detection of  $Na^{+}$  and  $Mg^{+}$ , there are no adducts of organic fragments with these ions. However some of the organic fragments such as  $[Ade + H]^{+}$  are also detected. The smaller mass ions are present in both cases.

In negative mode presented in Figure 7-C and 7-D, the analysis gives us other informations. Without any salts in the sample, the deprotonated molecular ion is not detected, neither the adducts ones. Deprotonated ion of the Adenine [Ade-H]<sup>-</sup> is otherwise detectable, and is the higher  $m/z$  of the mass spectrum. A great diversity of low mass fragments is visible. This analysis allows to detect the C<sub>5</sub>H<sub>7</sub>O<sub>4</sub> fragment, corresponding to the Ribofuranose, which remains unseen in positive ion mode. Under salty environment (Figure 7-D), no adduct is detected, and no ion with  $m/z$  higher than [Ade-H]<sup>-</sup>. Few differences are visible. If Cl<sup>-</sup> is clearly visible, there are no adducts with this ion. The spectrum shows less peaks, half of the ions detected with the pure Adenosine sample are not detected with this sample; the Ribofuranose fragment seen without salts is not detected in this configuration.

These results show that LIMS experiments performed with a TRL5 CosmOrbitrap allows separation of organics ions from metal adducts, as well as precise identification of the fragments detected thanks to the high resolving power and mass accuracy. The presence of salts does not modify the detection capabilities of the instrument, but seems to favor the fragmentation process. However, presence of salts may induce adsorption processes in complex samples such as clay (Franchi et al., 2003).

In the case of this study, the positive and negative ion modes are complementary, the positive mode allows an unequivocal identification of the molecule initially present, while the negative mode brings information on the low mass ions created during the ablation.



- **Conclusion**

This paper presents first results in terms of instrumental performance of the LAB-CosmOrbitrap prototype with a ruggedized CosmOrbitrap TRL of 5 in dual polarity mode. The CosmOrbitrap

subsystem in negative ion mode allows detection of different compounds with a high mass resolution; this mass resolution is close to half of the maximum reachable by a D30 Orbitrap cell despite the simplicity of the instrumental configuration. The specific study of the relative abundance of major platinum isotopes showed RIA error lesser than 5 % for the 3 more abundant isotopes.

This work has demonstrated that the CosmOrbitrap, in its TRL5 version, could be a key component for any future space exploration mission with astrobiological objectives even if they are mixed with salt matrices. Its characteristics make it a subsystem that can be easily adapted for inclusion on board an orbiter as well as a lander.

### Acknowledgement

We thank all the people involved in the development of the CosmOrbitrap experiment, especially the CosmOrbitrap consortium and the CNES.

We gratefully acknowledged J.-P. Lebreton for his help for processing data and A. Makarov for his advices and suggestions about this work. We also thank the two anonymous reviewers for their helpful comments.

B.C. thanks the CNES and the French Région Centre-Val de Loire for the funding of his PhD.

### References

- Arevalo Jr., R., Selliez, L., Briois, C., Carrasco, N., Thirkell, L., Cherville, B., Colin, F., Gaubicher, B., Farcy, B., Li, X., Makarov, A., 2018. An Orbitrap-based laser desorption/ablation mass spectrometer designed for spaceflight. *Rapid Commun. Mass Spectrom.* 32, 1875–1886. <https://doi.org/10.1002/rcm.8244>
- Arevalo, R., Willhite, L., Bardyn, A., Ni, Z., Ray, S., Southard, A., Danell, R., Grubisic, A., Gundersen, C., Minasola, N., Yu, A., Fahey, M., Hernandez, E., Briois, C., Thirkell, L., Colin, F., Makarov, A., 2023. Laser desorption mass spectrometry with an Orbitrap analyser for in situ astrobiology. *Nat. Astron.* 1–7. <https://doi.org/10.1038/s41550-022-01866-x>

Azov, V.A., Mueller, L., Makarov, A.A., 2020. Laser Ionization Mass Spectrometry at 55: Quo Vadis? *Mass Spectrom. Rev.* 41, 100–151. <https://doi.org/10.1002/mas.21669>

Brenna, J.T., Creasy, W.R., 1989. Experimental evaluation of apodization functions for quantitative fourier transform mass spectrometry. *Int. J. Mass Spectrom. Ion Process.* 90, 151–166. [https://doi.org/10.1016/0168-1176\(89\)85005-0](https://doi.org/10.1016/0168-1176(89)85005-0)

Briois, C., Thissen, R., Thirkell, L., Aradj, K., Bouabdellah, A., Boukrara, A., Carrasco, N., Chalumeau, G., Chapelon, O., Colin, F., Coll, P., Cottin, H., Engrand, C., Grand, N., Lebreton, J.-P., Orthous-Daunay, F.-R., Pennanech, C., Szopa, C., Vuitton, V., Zapf, P., Makarov, A., 2016. Orbitrap mass analyser for in situ characterisation of planetary environments: Performance evaluation of a laboratory prototype. *Planet. Space Sci.* 131, 33–45. <https://doi.org/10.1016/j.pss.2016.06.012>

Brown, M.E., Hand, K.P., 2013. SALTS AND RADIATION PRODUCTS ON THE SURFACE OF EUROPA. *Astron. J.* 145, 110. <https://doi.org/10.1088/0004-6256/145/4/110>

Camprubí, E., de Leeuw, J.W., House, C.H., Raulin, F., Russell, M.J., Spang, A., Tirumalai, M.R., Westall, F., 2019. The Emergence of Life. *Space Sci. Rev.* 215, 56. <https://doi.org/10.1007/s11214-019-0624-8>

Choblet, G., Tobie, G., Buch, A., Čadek, O., Barge, L.M., Běhouňková, M., Camprubi, E., Freissinet, C., Hedman, M., Jones, G., Lainey, V., Le Gall, A., Lucchetti, A., MacKenzie, S., Mitri, G., Neveu, M., Nimmo, F., Olsson-Francis, K., Panning, M., Postberg, F., Saur, J., Schmidt, J., Sekine, Y., Shibuya, T., Sotin, C., Soucek, O., Szopa, C., Usui, T., Vance, S., Van Hoolst, T., 2021. Enceladus as a potential oasis for life: Science goals and investigations for future explorations. *Exp. Astron.* <https://doi.org/10.1007/s10686-021-09808-7>

Coustenis, A., Atreya, S.K., Balint, T., Brown, R.H., Dougherty, M.K., Ferri, F., Fulchignoni, M., Gautier, D., Gowen, R.A., Griffith, C.A., Gurvits, L.I., Jaumann, R., Langevin, Y., Leese, M.R., Lunine, J.I., McKay, C.P., Moussas, X., Müller-Wodarg, I., Neubauer, F., Owen, T.C., Raulin, F., Sittler, E.C., Sohl, F., Sotin, C., Tobie, G., Tokano, T., Turtle, E.P., Wahlund, J.-E., Waite, J.H., Baines, K.H., Blamont, J., Coates, A.J., Dandouras, I., Krimigis, T., Lellouch, E., Lorenz, R.D., Morse, A., Porco, C.C., Hirtzig, M., Saur, J., Spilker, T., Zarnecki, J.C., Choi, E., Achilleos, N., Amils, R., Annan, P., Atkinson, D.H., Bénilan, Y., Bertucci, C., Bézard, B., Bjoraker, G.L., Blanc, M., Boireau, L., Bouman, J., Cabane, M., Capria, M.T., Chassefière, E., Coll, P., Combes, M., Cooper, J.F., Coradini, A., Crary, F., Cravens, T., Daglis, I.A., de Angelis, E., de Bergh, C., de Pater, I., Dunford, C., Durry, G., Dutuit, O., Fairbrother, D., Flasar, F.M., Fortes, A.D., Frampton, R., Fujimoto, M., Galand, M., Grasset, O., Grott, M., Haltigin, T., Herique, A., Hersant, F., Hussmann, H., Ip, W., Johnson, R., Kallio, E., Kempf, S., Knapmeyer, M., Kofman, W., Koop, R., Kostiuik, T., Krupp, N., Küppers, M., Lammer, H., Lara, L.-M., Lavvas, P., Le Mouélic, S., Lebonnois, S., Ledvina, S., Li, J., Livengood, T.A., Lopes, R.M., Lopez-Moreno, J.-J., Luz, D., Mahaffy, P.R., Mall, U., Martinez-Frias, J., Marty, B., McCord, T., Menor Salvan, C., Milillo, A., Mitchell, D.G., Modolo, R., Mousis, O., Nakamura, M., Neish, C.D., Nixon, C.A., Nna Mvondo, D., Orton, G., Paetzold, M., Pitman, J., Pogrebenko, S., Pollard, W., Prieto-Ballesteros, O., Rannou, P., Reh, K., Richter, L., Robb, F.T., Rodrigo, R., Rodriguez, S., Romani, P., Ruiz Bermejo, M., Sarris, E.T., Schenk, P., Schmitt, B., Schmitz, N., Schulze-Makuch, D., Schwingenschuh, K., Selig, A., Sicardy, B., Soderblom, L., Spilker, L.J., Stam, D., Steele, A., Stephan, K., Strobel, D.F., Szego, K., Szopa, C., Thissen, R., Tomasko, M.G., Toubanc, D., Vali, H., Vardavas, I., Vuitton, V., West, R.A., Yelle, R., Young, E.F., 2009. TandEM: Titan and Enceladus mission. *Exp. Astron.* 23, 893–946. <https://doi.org/10.1007/s10686-008-9103-z>

- Franchi, M., Ferris, J.P., Gallori, E., 2003. Cations as mediators of the adsorption of nucleic acids on clay surfaces in prebiotic environments. *Orig. Life Evol. Biosphere J. Int. Soc. Study Orig. Life* 33, 1–16. <https://doi.org/10.1023/a:1023982008714>
- Grasset, O., Dougherty, M.K., Coustenis, A., Bunce, E.J., Erd, C., Titov, D., Blanc, M., Coates, A., Drossart, P., Fletcher, L.N., Hussmann, H., Jaumann, R., Krupp, N., Lebreton, J.-P., Prieto-Ballesteros, O., Tortora, P., Tosi, F., Van Hoolst, T., 2013. JUPITER ICY moons Explorer (JUICE): An ESA mission to orbit Ganymede and to characterise the Jupiter system. *Planet. Space Sci.* 78, 1–21. <https://doi.org/10.1016/j.pss.2012.12.002>
- Hand, K., Sotin, C., Hayes, A., Coustenis, A., 2020. On the Habitability and Future Exploration of Ocean Worlds. *Space Sci. Rev.* 216. <https://doi.org/10.1007/s11214-020-00713-7>
- Hendrix, A.R., Hurford, T.A., Barge, L.M., Bland, M.T., Bowman, J.S., Brinckerhoff, W., Buratti, B.J., Cable, M.L., Castillo-Rogez, J., Collins, G.C., Diniega, S., German, C.R., Hayes, A.G., Hoehler, T., Hosseini, S., Howett, C.J.A., McEwen, A.S., Neish, C.D., Neveu, M., Nordheim, T.A., Patterson, G.W., Patthoff, D.A., Phillips, C., Rhoden, A., Schmidt, B.E., Singer, K.N., Soderblom, J.M., Vance, S.D., 2019. The NASA Roadmap to Ocean Worlds. *Astrobiology* 19, 1–27. <https://doi.org/10.1089/ast.2018.1955>
- Howell, S.M., Pappalardo, R.T., 2020. NASA's Europa Clipper—a mission to a potentially habitable ocean world. *Nat. Commun.* 11, 1311. <https://doi.org/10.1038/s41467-020-15160-9>
- Hussmann, H., Sohl, F., Spohn, T., 2006. Subsurface oceans and deep interiors of medium-sized outer planet satellites and large trans-neptunian objects. *Icarus* 185, 258–273. <https://doi.org/10.1016/j.icarus.2006.06.005>
- Johnson, B.W., Wing, B.A., 2020. Limited Archaean continental emergence reflected in an early Archaean 18O-enriched ocean. *Nat. Geosci.* 13, 243–248. <https://doi.org/10.1038/s41561-020-0538-9>
- Khurana, K.K., Kivelson, M.G., Stevenson, D.J., Schubert, G., Russell, C.T., Walker, R.J., Polansky, C., 1998. Induced magnetic fields as evidence for subsurface oceans in Europa and Callisto. *Nature* 395, 777–780. <https://doi.org/10.1038/27394>
- Kind, T., Fiehn, O., 2006. Metabolomic database annotations via query of elemental compositions: Mass accuracy is insufficient even at less than 1 ppm. *BMC Bioinformatics* 7, 234. <https://doi.org/10.1186/1471-2105-7-234>
- Kivelson, M.G., Khurana, K.K., Russell, C.T., Volwerk, M., Walker, R.J., Zimmer, C., 2000. Galileo Magnetometer Measurements: A Stronger Case for a Subsurface Ocean at Europa. *Science* 289, 1340–1343. <https://doi.org/10.1126/science.289.5483.1340>
- Knolhoff, A.M., Callahan, J.H., Croley, T.R., 2014. Mass Accuracy and Isotopic Abundance Measurements for HR-MS Instrumentation: Capabilities for Non-Targeted Analyses. *J. Am. Soc. Mass Spectrom.* 25, 1285–1294. <https://doi.org/10.1021/jasms.8b04805>
- Ligier, N., Poulet, F., Carter, J., Brunetto, R., Gourgéot, F., 2016. VLT/SINFONI OBSERVATIONS OF EUROPA: NEW INSIGHTS INTO THE SURFACE COMPOSITION. *Astron. J.* 151, 163. <https://doi.org/10.3847/0004-6256/151/6/163>
- MacKenzie, S., Neveu, M., Davila, A., Lunine, J., Craft, K., Cable, M., Phillips-Lander, C., Hofgartner, J., Eigenbrode, J., Waite, J., Glein, C., Gold, R., Greenauer, P., Kirby, K., Bradburne, C., Kounaves, S., Malaska, M., Postberg, F., Patterson, G., Spilker, L., 2021. The Enceladus Orbilander Mission Concept:

Balancing Return and Resources in the Search for Life. *Planet. Sci. J.* 2, 77. <https://doi.org/10.3847/PSJ/abe4da>

Makarov, A., 2000. Electrostatic Axially Harmonic Orbital Trapping: A High-Performance Technique of Mass Analysis. *Anal. Chem.* 72, 1156–1162. <https://doi.org/10.1021/ac991131p>

Makarov, A., Denisov, E., Lange, O., 2009. Performance evaluation of a high-field orbitrap mass analyzer. *J. Am. Soc. Mass Spectrom.* 20, 1391–1396. <https://doi.org/10.1016/j.jasms.2009.01.005>

Mitri, G., Barnes, J., Coustenis, A., Flamini, E., Hayes, A., Lorenz, R.D., Mastrogiuseppe, M., Orosei, R., Postberg, F., Reh, K., Soderblom, J.M., Sotin, C., Tobie, G., Tortora, P., Vuitton, V., Wurz, P., 2021. Exploration of Enceladus and Titan: investigating ocean worlds' evolution and habitability in the Saturn system. *Exp. Astron.* <https://doi.org/10.1007/s10686-021-09772-2>

Myers, R.T., 1990. The periodicity of electron affinity. *J. Chem. Educ.* 67, 307. <https://doi.org/10.1021/ed067p307>

Nimmo, F., Hamilton, D.P., McKinnon, W.B., Schenk, P.M., Binzel, R.P., Bierson, C.J., Beyer, R.A., Moore, J.M., Stern, S.A., Weaver, H.A., Olkin, C.B., Young, L.A., Smith, K.E., New Horizons Geology, Geophysics & Imaging Theme Team, 2016. Reorientation of Sputnik Planitia implies a subsurface ocean on Pluto. *Nature* 540, 94–96. <https://doi.org/10.1038/nature20148>

Pappalardo, R.T., Belton, M.J.S., Breneman, H.H., Carr, M.H., Chapman, C.R., Collins, G.C., Denk, T., Fagents, S., Geissler, P.E., Giese, B., Greeley, R., Greenberg, R., Head, J.W., Helfenstein, P., Hoppa, G., Kadel, S.D., Klaasen, K.P., Klemaszewski, J.E., Magee, K., McEwen, A.S., Moore, J.M., Moore, W.B., Neukum, G., Phillips, C.B., Prockter, L.M., Schubert, G., Senske, D.A., Sullivan, R.J., Tufts, B.R., Turtle, E.P., Wagner, R., Williams, K.K., 1999. Does Europa have a subsurface ocean? Evaluation of the geological evidence. *J. Geophys. Res. Planets* 104, 24015–24055. <https://doi.org/10.1029/1998JE000628>

Perry, R.H., Cooks, R.G., Noll, R.J., 2008. Orbitrap mass spectrometry: Instrumentation, ion motion and applications. *Mass Spectrom. Rev.* 27, 661–699. <https://doi.org/10.1002/mas.20186>

Postberg, F., Khawaja, N., Abel, B., Choblet, G., Glein, C.R., Gudipati, M.S., Henderson, B.L., Hsu, H.-W., Kempf, S., Klenner, F., Moragas-Klostermeyer, G., Magee, B., Nölle, L., Perry, M., Reviol, R., Schmidt, J., Srama, R., Stolz, F., Tobie, G., Trieloff, M., Waite, J.H., 2018. Macromolecular organic compounds from the depths of Enceladus. *Nature* 558, 564–568. <https://doi.org/10.1038/s41586-018-0246-4>

Reh, K., Spilker, L., Lunine, J.I., Waite, J.H., Cable, M.L., Postberg, F., Clark, K., 2016. Enceladus Life Finder: The search for life in a habitable Moon, in: 2016 IEEE Aerospace Conference. Presented at the 2016 IEEE Aerospace Conference, IEEE, Big Sky, MT, USA, pp. 1–8. <https://doi.org/10.1109/AERO.2016.7500813>

Saur, J., Duling, S., Roth, L., Jia, X., Strobel, D.F., Feldman, P.D., Christensen, U.R., Retherford, K.D., McGrath, M.A., Musacchio, F., Wennmacher, A., Neubauer, F.M., Simon, S., Hartkorn, O., 2015. The search for a subsurface ocean in Ganymede with Hubble Space Telescope observations of its auroral ovals. *J. Geophys. Res. Space Phys.* 120, 1715–1737. <https://doi.org/10.1002/2014JA020778>

Selliez, L., Briois, C., Carrasco, N., Thirkell, L., Thissen, R., Ito, M., Orthous-Daunay, F.-R., Chalumeau, G., Colin, F., Cottin, H., Engrand, C., Flandinet, L., Fray, N., Gaubicher, B., Grand, N., Lebreton, J.-P., Makarov, A., Ruocco, S., Szopa, C., Vuitton, V., Zapf, P., 2019. Identification of organic molecules

with a laboratory prototype based on the Laser Ablation-CosmOrbitrap. *Planet. Space Sci.* 170, 42–51. <https://doi.org/10.1016/j.pss.2019.03.003>

Selliez, L., Maillard, J., Cherville, B., Gautier, T., Thirkell, L., Gaubicher, B., Schmitz-Afonso, I., Afonso, C., Briois, C., Carrasco, N., 2020. High-resolution mass spectrometry for future space missions: Comparative analysis of complex organic matter with LAB-CosmOrbitrap and laser desorption/ionization Fourier transform ion cyclotron resonance. *Rapid Commun. Mass Spectrom.* 34, e8645. <https://doi.org/10.1002/rcm.8645>

Somogyi, Á., Smith, M.A., Vuitton, V., Thissen, R., Komáromi, I., 2012. Chemical ionization in the atmosphere? A model study on negatively charged “exotic” ions generated from Titan’s tholins by ultrahigh resolution MS and MS/MS. *Int. J. Mass Spectrom., Special Issue Honoring Alex G. Harrison on the Occasion of his 80th Birthday: Structures, Reactions, and Thermochemistry of Gas-Phase Ions* 316–318, 157–163. <https://doi.org/10.1016/j.ijms.2012.02.026>

Sulaiman, A.H., Achilleos, N., Bertucci, C., Coates, A., Dougherty, M., Hadid, L., Holmberg, M., Hsu, H.-W., Kimura, T., Kurth, W., Gall, A.L., McKeivitt, J., Morooka, M., Murakami, G., Regoli, L., Roussos, E., Saur, J., Shebanits, O., Solomonidou, A., Wahlund, J.-E., Waite, J.H., 2021. Enceladus and Titan: emerging worlds of the Solar System. *Exp. Astron.* <https://doi.org/10.1007/s10686-021-09810-z>

Tobie, G., Teanby, N.A., Coustenis, A., Jaumann, R., Raulin, F., Schmidt, J., Carrasco, N., Coates, A.J., Cordier, D., De Kok, R., Geppert, W.D., Lebreton, J.-P., Lefevre, A., Livengood, T.A., Mandt, K.E., Mitri, G., Nimmo, F., Nixon, C.A., Norman, L., Pappalardo, R.T., Postberg, F., Rodriguez, S., Schulze-Makuch, D., Soderblom, J.M., Solomonidou, A., Stephan, K., Stofan, E.R., Turtle, E.P., Wagner, R.J., West, R.A., Westlake, J.H., 2014. Science goals and mission concept for the future exploration of Titan and Enceladus. *Planet. Space Sci.* 104, part A, 59–77. <https://doi.org/10.1016/j.pss.2014.10.002>

Trumbo, S.K., Brown, M.E., Hand, K.P., 2019. Sodium chloride on the surface of Europa. *Sci. Adv.* 5, eaaw7123. <https://doi.org/10.1126/sciadv.aaw7123>

Tsou, P., Brownlee, D.E., McKay, C.P., Anbar, A.D., Yano, H., Altwegg, K., Beegle, L.W., Dissly, R., Strange, N.J., Kanik, I., 2012. LIFE: Life Investigation For Enceladus A Sample Return Mission Concept in Search for Evidence of Life. *Astrobiology* 12, 730–742. <https://doi.org/10.1089/ast.2011.0813>

Waite, J.H., Glein, C.R., Perryman, R.S., Teolis, B.D., Magee, B.A., Miller, G., Grimes, J., Perry, M.E., Miller, K.E., Bouquet, A., Lunine, J.I., Brockwell, T., Bolton, S.J., 2017. Cassini finds molecular hydrogen in the Enceladus plume: Evidence for hydrothermal processes. *Science* 356, 155–159. <https://doi.org/10.1126/science.aai8703>

Waite, J.H., Young, D.T., Cravens, T.E., Coates, A.J., Crary, F.J., Magee, B., Westlake, J., 2007. The Process of Tholin Formation in Titan’s Upper Atmosphere. *Science* 316, 870–875. <https://doi.org/10.1126/science.1139727>

Waite Jr, J.H., Lewis, W.S., Magee, B.A., Lunine, J.I., McKinnon, W.B., Glein, C.R., Mousis, O., Young, D.T., Brockwell, T., Westlake, J., Nguyen, M.-J., Teolis, B.D., Niemann, H.B., McNutt Jr, R.L., Perry, M., Ip, W.-H., 2009. Liquid water on Enceladus from observations of ammonia and 40Ar in the plume. *Nature* 460, 487–490. <https://doi.org/10.1038/nature08153>

Xu, Y., Heilier, J.-F., Madalinski, G., Genin, E., Ezan, E., Tabet, J.-C., Junot, C., 2010. Evaluation of Accurate Mass and Relative Isotopic Abundance Measurements in the LTQ-Orbitrap Mass Spectrometer for Further Metabolomics Database Building. *Anal. Chem.* 82, 5490–5501. <https://doi.org/10.1021/ac100271j>

- Negative ion mode capabilities characterization of the CosmOrbitrap mass analyser
- First data from the laser-CosmOrbitrap instrument in its TRL5 configuration
- Organic molecule mixed with salts identification with the LAb-CosmOrbitrap instrument

Journal Pre-proof

Dear editor,

Thank you for considering our work to be published.

We considered the reviewers comments as well as possible give you this new version of our paper. We hope that it will suit your publication requirements, and we look forward to receiving your final answer.

Best regards,

Barnabé Cherville

Journal Pre-proof

**Declaration of interests**

The authors declare that they have no known competing financial interests or personal relationships that could have appeared to influence the work reported in this paper.

The authors declare the following financial interests/personal relationships which may be considered as potential competing interests:

Journal Pre-proof